

A GENERALIZED DYNAMIC LINEAR MODEL  
OF A CONVERTER - FED DC MOTOR SYSTEM

BY  
M. M. ATOUT and S. A. MAHMOUD  
Helwan University, Menoufia University,  
Helwan - Cairo- Egypt. Shebin El-Kom, Egypt.

ABSTRACT:

This paper deals with an AC-DC power conversion unit connected to a separately excited DC motor drive system, and supplied by an AC feeder line. A generalized linear mathematical model of such a system is developed, which represents the equations describing the system dynamic behaviour. The converter current controller and the DC motor speed controller are presented, and the model is valid for any type of such controllers. The developed model represents different configurations of the converter operation; it is also applicable to any type of AC - DC converter supplying a separately excited DC motor, and it is suitable for any mode of converter operation.

The analysis is based on perturbation technique method, and the system with their controllers are represented by a signal flow graph. This permits the evaluation of transfer functions of the overall system for a step change in the control reference parameters (speed reference and load torque). Then, the time responses of the motor speed and the armature current can be determined.

An application is considered for a separately excited DC motor fed by a single phase bridge rectifier. A comparison is made between the experimental and theoretical results.

1. INTRODUCTION:

Direct current drives are extensively used in industry. The outstanding advantages of DC drives, such as ease of control, precise and continuous

control of speed over a wide range ensure their popularity. When designing a high response thyristor drive with internal multicontrol loops, the transient behaviour must be taken into consideration to achieve the required dynamic performance.

The design, construction and testing of a closed-loop system for the speed control of a separately excited DC motor fed from dual converter are well discussed in literature [1]. The perturbation technique has been used for the transient analysis of a controlled bridge rectifier with a DC motor load [2-4]. A microprocessor implementation is proposed to study the effect of discontinuous conduction on a converter-fed DC drive [5]. The application of dynamic optimal control theory on typical industrial speed-controlled DC machine drives reveals the manner in which the control should operate [6]. Three different methods to calculate the current and speed controller parameters for a DC motor fed from a single-phase thyristor bridge have been presented [7,8].

In this paper, a generalized mathematical linear model of a separately excited DC motor supplied from an AC-DC converter is presented. The dynamic model allows us to obtain the time responses of the motor speed and armature current for a step change in the control reference parameters.

In the model, different configurations of converter operation are considered: the load current continuity, the presence of freewheeling diode across the motor terminals, the type of the AC feeder, the type of rectifier elements and the mode of rectification.

The analysis is based on perturbation technique method; and the overall system is represented in the form of signal flow graph. Experimental and theoretical results are compared for a single phase bridge rectifier with a DC motor load.

## 2. SIGNAL FLOW GRAPHS OF SYSTEM ELEMENTS:

The dynamic simulation of a separately excited DC motor fed by a thyristorized converter is presented. With the application of perturbation technique method on the equations representing the steady state operation of the system elements, the incremental variations of the variables of each element can be obtained.

### 2.1 DC motor:

The armature voltage and the torque balance equations are:

$$v_d = k_e \phi n_m + R_a i_a + L_m (di_a/dt) \quad (1)$$

$$k_t \phi i_a = T_L + B i_a + J (dn_m/dt) \quad (2)$$

consider that the motor mechanical time constant is greater than the electrical time constant; and for small perturbations in the motor variables, the incremental equations are:

$$\Delta I_a = A_1 \Delta V_d + B_1 \Delta N_m \quad (3)$$

$$\Delta N_m = C \Delta I_a + D \Delta T_L \quad (4)$$

where the constants  $A_1, B_1, C$  and  $D$  are functions of the nominal values  $I_a, N_m, T_L, V_d$  and  $T_e$ .

The signal flow graph is shown in Figure (1).

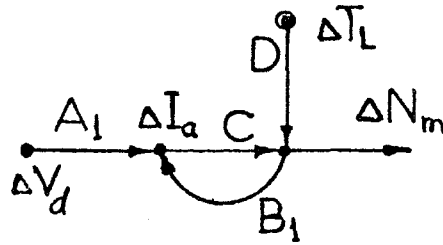
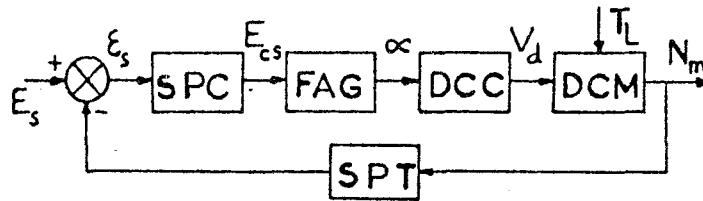


Figure (1): Motor signal flow graph.

## 2.2 Closed loop speed controller:

In most applications, the armature voltage of the motor is controlled in a closed loop feedback system. The schematic diagram of the motor speed controller associated with the converter-motor is shown in Figure (2).



SPC = Speed controller, DCC = Direct current converter,  
 FAG = Firing angle pulse generator, DCM = DC motor  
 SPT = Motor speed transducer.

Figure (2): Speed Controller diagram.

The speed controller is represented by the generalized transfer function  $G(s)$ , which can be a proportional type or proportional-integral type. The firing angle pulse generator is represented by a cosine function related to the output voltage of the DC converter.

The incremental variations of the speed control circuit are defined by:

$$\Delta E_{cs} = F \Delta E_s + F_N \Delta N_m \quad (5)$$

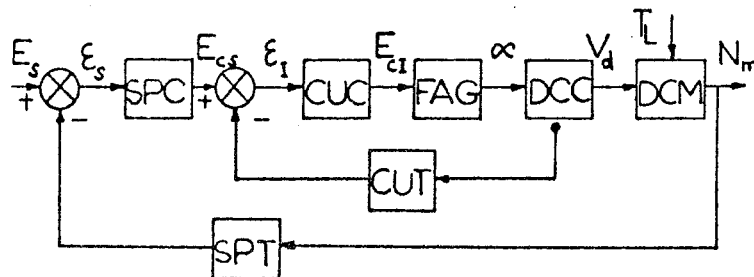
$$\Delta \alpha = T_1 \Delta E_{cs} \quad (6)$$

where,  $F$  and  $F_N$  are the transfer functions of the speed controller and speed transducer, respectively.

$T_1$  represents the pulse generator transfer function.

### 2.3 Closed loop current controller:

An inner current limiting control loop is incorporated as a protective feature, and the clamped speed error is used as a current reference. The schematic diagram of the overall system is shown in Figure (3).



CUC = Current controller , CUT = Current transducer

Figure (3): Control loop diagram.

The current controller is represented by its generalized transfer function  $G_I(s)$ , which may be simulated as a proportional type or proportional-integral type.

The incremental variations of the current control loop are defined by:

$$\Delta E_{cI} = F_1 \cdot \Delta E_{cs} + F_{1I} \cdot \Delta I_a \quad (7)$$

$$\Delta \alpha = T_2 \cdot \Delta E_{cI} \quad (8)$$

where,  $F_1$  and  $F_{1I}$  are the transfer functions of the current controller and current transducer.

$T_2$  represents the pulse generator transfer function.

The signal flow graph of the system is shown in Figure (4).

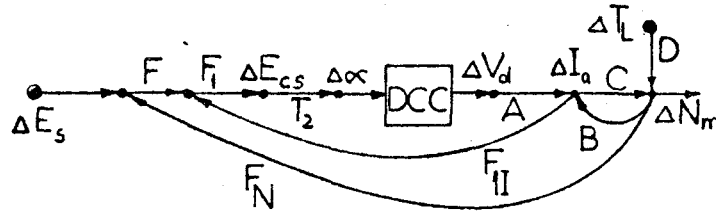


Figure (4): System signal flow graph.

#### 2.4 AC-DC converter:

In this section, the signal flow graph which shows the relation between the incremental variations  $\Delta V_d$  and  $\Delta \alpha$ , will be determined.

An attempt is made to analyse all possible modes of steady state operation for different types of AC-DC converters; this permits a general form definition of the average motor terminal voltage:

$$V_d = (\sqrt{2} V / 2\pi/qh_w) [h_\alpha q \cos(\alpha + h_q \frac{\pi}{6}) + h_\pi \cos \{ \pi + h_f h_d (\beta + h_q \frac{\pi}{6}) \} + h_d^m \{ (2\pi/qh_w) + (\alpha - \beta) \}] \quad (9)$$

and the general form of the equation which permits evaluation of the extinction angle  $\beta$  is given by:

$$\begin{aligned} & \sin \{ \pi + h_f (\beta - \pi) + h_q \frac{\pi}{6} - \phi \} \\ & \frac{(\beta + h_q \frac{\pi}{6} - \pi) (1 - h_f)}{\tan \phi} \frac{\alpha - \pi - h_f (\beta - \pi)}{\tan} \\ = & \frac{m}{\cos \phi} [ e^{-\frac{\alpha - \pi - h_f (\beta - \pi)}{\tan \phi}} \\ & + \sin (\alpha + h_q \frac{\pi}{6} - \phi) e \quad (10) \end{aligned}$$

where,  $q$  defines the type of the AC feeder (single or three phase).

$h_w$  defines the type of the output DC voltage waveform (half wave or fullwave).  
 $h_d$  defines the armature current continuity.  
 $h_f$  defines the presence of the freewheeling diode across the motor terminals.  
 $h_\alpha, h_\pi$  and  $h_q$  define some different modes of converter operation for the previous cases.

The following table summarizes the different types and modes of converter operation, and the values of the definition parameters are indicated.

	Single phase												Three phase								
	half wave						full wave						half wave			full wave					
	fully controlled FC						half controlled NF			fully controlled EC			fully controlled EC			HC		FC			
	TF	WF	TF	WF	TF	WF	TF	WF	TF	WF	TF	WF	TF	WF	WF	TF					
D	DN	C	D	C	D	DN	C	D	C	D	DN	C	D	C	D	C	C				
$q$	1	1	1	1	1	1	1	1	1	1	1	1	1	3	3	3	3	3	3	3	
$h_w$	1	1	1	1	2	2	2	2	2	2	2	2	2	1	1	1	1	1	1	1	2
$h_d$	1	1	1	0	1	0	1	1	0	1	1	0	1	0	1	1	0	1	0	0	0
$h_f$	1	0	1	0	0	0	1	0	1	1	0	1	0	1	1	0	1	0	0	0	1
$h_\alpha$	1	1	1	1	1	1	1	1	1	4	1	1	1	1/3	1	1/3	1/3	1/3	1	1	1
$h_\pi$	1	-1	1	-1	-1	-1	1	-1	1	0	-1	1	-1	1	0	-1	1	-1	-1	-1	0
$h_q$	0	0	0	0	0	0	0	0	0	0	0	0	0	1	0	1	1	1	0	0	0

HC half controlled , FC fully controlled  
 TF without freewheeling diode, WF with freewheeling diode  
 D discontinuous current C continuous current,  
 DN discontinuous and the freewheeling diode not conducting.

The general form of the incremental variations of the the variables describing the operation of the converter is:

$$\Delta V_d = W_1 \Delta \alpha + W_2 \Delta N_m + W_3 \Delta \beta \quad (11)$$

$$\Delta \beta = W_4 \Delta \alpha + W_5 \Delta N_m \quad (12)$$

where,

$$W_1 = \frac{h_d E_a - \sqrt{2/q} h_\alpha V \sin(\alpha + h_q \frac{\pi}{6})}{V_d} \quad \frac{\alpha}{2\pi/q h_w}$$

$$W_3 = h_d \frac{-h_f h_f / \sqrt{2V} \sin\{\pi + h_f h_d (\beta + h_q \frac{\pi}{6})\} - E_a \beta}{V_d \cdot 2\pi / q h_w}$$

$$W_2 = h_d \frac{\{(2\pi / q h_w) + (\alpha - \beta)\} E_a}{(2\pi / q h_w) V_d}$$

$$W_4 = h_d \frac{\cos\{\alpha + h_q \frac{\pi}{6} - \phi\} e^{\frac{\alpha - \pi - h_f (\beta - \pi)}{\tan \phi}}}{\cos\{\pi + h_f (\beta - \pi) + h_q \frac{\pi}{6} - \phi\} e^{\frac{\alpha - \pi - h_f (\beta - \pi)}{\tan \phi}}}$$

$$W_5 = h_d \frac{e^{(\beta + h_q \frac{\pi}{6} - \pi) (1 - h_f)} \frac{\alpha - \pi - h_f (\beta - \pi)}{\tan \phi} E_a}{\cos\{\pi + h_f (\beta - \pi) + h_q \frac{\pi}{6} - \phi\} \beta / \sqrt{2V} \cos \phi}$$

The general form of the signal flow graph is shown in Figure (5):

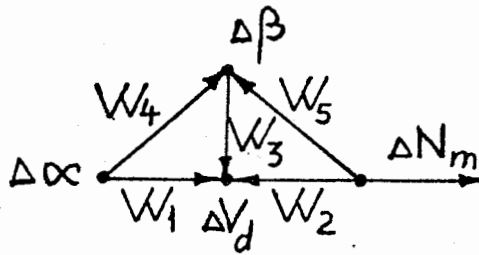


Figure (5): Signal flow graph of converter.

The values of  $W_1 : W_5$  are determined, depending on the converter type and the nature of its mode of operation.

### 3. CONVERTER-MOTOR SYSTEM RESPONSES:

The signal flow graph representing the dynamic operation of the AC-DC converter and the separately excited DC motor load with the associated control loops is shown in Figure (6).

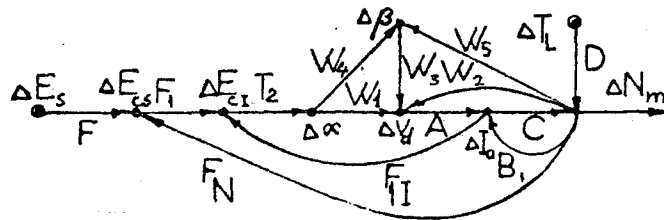


Figure (6): System signal flow graph.

The signal flow graph theory permits eliminating the intermediate nodes in order to obtain a direct relation between the output and input nodes [9]. Then, the transfer functions  $\Delta N_m / \Delta E_s$ ,  $\Delta N_m / \Delta T_L$ ,  $\Delta I_a / \Delta E_s$  and  $\Delta I_a / \Delta T_L$  are determined; and the time responses can be evaluated when either a step change in the speed reference or in the load torque.

#### 4. RESULTS:

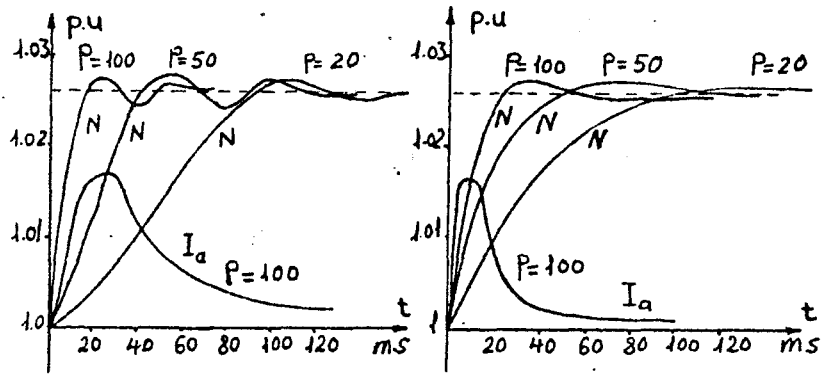
The model responses for a step change in the speed reference of a single phase converter connected to a separately excited DC motor are obtained.

Figure (7) shows the speed and current responses for continuous and discontinuous current operation.

The experimental responses of current and speed have been recorded in the linear operating mode, by giving a small step change in the speed reference signal of the speed controller. Figure (8) shows photographs of the speed response for two different values of the controller gain.

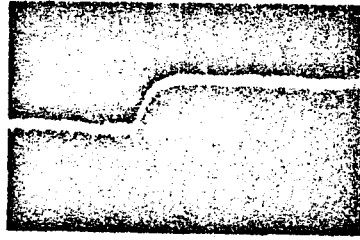
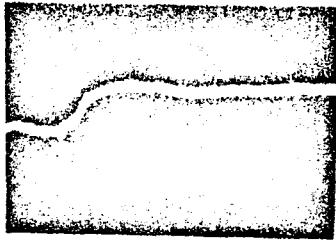
Figure (9) shows the experimental time response of the armature current. The experimental results verify the validity of the proposed mathematical model representing the system dynamic operation.





a- Continuous current.    b- Discontinuous current.

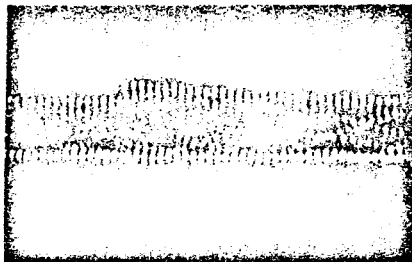
Figure (7): Time responses of current and speed for step change in speed reference.



a-  $K = 0.0209$

b-  $K = 0.1239$

Figure (8): Experimental speed response.



$K = 0.0209$

Figure (9): Experimental current response.

### 5. CONCLUSION:

The generalized dynamic linear model given in this paper is adaptable for different types of converter with different modes of operation. Good correlation between computed and experimental responses confirms that the model is valid for predicting the behaviour of a given system.

### 6. LIST OF SYMPOLS:

$i_a$	Instantaneous armature current (A)
$I_a$	Average value of armature current (A)
$v_d$	Instantaneous converter output voltage (V)
$V_d$	Average value of converter output voltage (V)
$E_{cs}$	Control voltage of the speed (V)
$E_{cI}$	Control voltage of the current (V)
$E_s$	Speed reference voltage (V)
$n_m$	Instantaneous motor speed (RPM)
$N_m$	Average value of motor speed. (RPM)
$T_L$	Load torque (M.m)
$K_t \phi$	Torque constant (N.m/A)
$K_e \phi$	Motor E.M.F constant (V/RPM)
$R_a, L_m$	Armature resistance and inductance
$J$	Inertia of the motor and coupled system $K_{gm}^2$
$B$	Viscous friction coefficient $N.m/red. Sec^{-1}$
$\alpha$	Thyristor firing angle
$\beta$	Thyristor extinction angle
$\Delta$	Incremental variation
$\epsilon_s, \epsilon_I$	Speed and current error.

### 7. SYSTEM PARAMETERS:

The system parameters in this work had the following values:

$P = 2.2 \text{ KW}$  ;  $N = 1500 \text{ rpm.}$   
 $K_e \phi = 0.518 (2 / 60)$  ;  $K_t \phi = 0.518$

a- continuous current

b- Discontinuous

$L_m$	0.09	H	0.08	H
$R_a$	1.65	ohm	3.45	ohm
$J$	0.01985	Kg m <sup>2</sup>	3.46	Kg.m <sup>2</sup>
$B$	0.0055	Nm/rad.Sec <sup>-1</sup>	0.029	Nm/rad.Sec. <sup>-1</sup>
$I_a$	11.32	A	8.944	A
$V_d$	100	V	112.2	V
$T_L$	5	Nm	0.08	Nm
$\alpha$	58°		128°	
$\beta$	238°		198°	

### 8. REFERENCES:

- [1] T.Krishnan and B.Ramaswami, "Speed control of DC motor using thyristor dual converter", IEEE, Vol. IECI-23, No. 4, Nov. 1976.
- [2] M.M.Atout, "Transient analysis of synchronous alternator connected to a controlled bridge rectifier with a DC motor load", ICEM proceeding, Budapest, 5:8 September 1982, PP. 559:562.
- [3] M.M.ATout, S.H.Shehab and F.I.Ahmed, "Analysis of transient response in thyristor controlled DC motor drives", UPEC'86 conference, Imperial college, London, April, 1986.
- [4] S.A.Mahmoud, "D.C. motor loaded synchronous generator Via fully controlled bridge rectifier", UPEC'81, conference, Sheffield, England, April, 1981.
- [5] D.Joos and E.D.Goodman, "Design consideration of an adaptive controller for DC drives", UPEC'84 conference, England, April 1984.
- [6] B.J. Cardwell and C.J. Goodman, "Response improvements in industrial DC drives derived from optimal analysis", IEE proceedings, Vol. 131, Pt.B, No. 3, May 1984, PP. 91:98.
- [7] A.S.Abdel-Ghaffar, A.A.El-Hefnawy, S.A.Mahmoud and S.A.Hassan, "Linear and non-linear modeling of speed and current control of DC motors", Fourth IASTED Int. Sym. Modelling, Lausanne, February, 1985.
- [8] A.S.Abdel-Ghaffar, S.A.Mahmoud, A.A.El-Hefnawy and S.A.Hassam, "Comparison between exact and simplified non-linear models of speed control of DC motor", Fourth IASTED Int. Sym. Modelling, Lausanne, February, 1985.

- [9] M.M. Atout and S.A. Mahmoud, "Reduction de graphe de fluence par ordinateur", 15<sup>th</sup> annual conf. in statistics and computer sciences, Cairo, University, Cairo, Egypt, December, 1980.

### 9. APPENDIX:

The transfer function of the signal flow graph

a- DC motor:

$$A_1 = (V_d / I_a R_a) \cdot (1 / (1 + \tau_e s)) \quad ; \quad B_1 = (-E_a / I_a R_a) \cdot (1 / (1 + \tau_e s))$$

$$C = (T_e / B N_m) \cdot (1 / (1 + \tau_m s)) \quad ; \quad D = (-T_L / B N_m) \cdot (1 / (1 + \tau_m s))$$

$$\tau_e = L_m / R_a \quad ; \quad \tau_m = J / B$$

b- Closed loop speed controller:

$$F = \frac{E_s}{E_{cs}} G_s (P) \quad ; \quad F_N = \frac{-A_2 N}{E_{cs}} G_s (P)$$

$$T_1 = \frac{-E_{cs}}{E_o \sin \alpha} \left( \frac{1}{\alpha} \right)$$

c- Closed loop current controller:

$$F_1 = \frac{E_{cs}}{E_{cI}} G_I (P) \quad ; \quad F_{1I} = \frac{-A_3 I_4}{E_{cI}} G_I (P)$$

$$T_2 = \frac{-E_{cI}}{E_o \sin \alpha} \left( \frac{1}{\alpha} \right)$$